Topological Transitions and Fractional Charges Induced by Strain and a Magnetic Field in Carbon Nanotubes

Yonathan Efroni,[1] Shahal Ilani,[1] and Erez Berg[1,2]
[1]Department of Condensed Matter Physics, Weizmann Institute of Science, Rehovot 7610001, Israel
[2]Department of Physics, James Frank Institute, University of Chicago, Chicago, Illinois 60637, USA
(Received 12 September 2016; revised manuscript received 15 July 2017; published 5 October 2017)

We show that carbon nanotubes (CNT) can be driven through a topological phase transition using either strain or a magnetic field. This can naturally lead to Jackiw-Rebbi soliton states carrying fractionalized charges, similar to those found in a domain wall in the Su-Schrieffer-Heeger model, in a setup with a spatially inhomogeneous strain and an axial field. Two types of fractionalized states can be formed at the interface between regions with different strain: a spin-charge separated state with integer charge and spin zero (or zero charge and spin $\pm\hbar/2$), and a state with charge $\pm e/2$ and spin $\pm\hbar/4$. The latter state requires spin-orbit coupling in the CNT. We show that in our setup, the precise quantization of the fractionalized interface charges is a consequence of the symmetry of the CNT under a combination of a spatial rotation by π and time reversal.

DOI: 10.1103/PhysRevLett.119.147704

Introduction.—Charge fractionalization is one of the most fascinating manifestations of emergent behavior in condensed matter physics. This phenomenon results from a subtle interplay of quantum many-body physics and topology. Although fractional charges were theoretically predicted to arise in different settings, only a handful of confirmed experimental realizations exist, the most prominent being fractional charges in quantum Hall states [1–4].

The earliest theoretical prediction of charge fractionalization was given by Jackiw and Rebbi [5] in the context of relativistic field theory. They showed that a one-dimensional (1D) Dirac equation with a spatially varying mass has a zero-energy eigenstate whenever the mass changes sign. This is a "half fermion" state, which carries a fermion charge of $e/2$ relative to the background filled Dirac sea. The solid state equivalent was suggested by Su, Schrieffer, and Heeger (SSH) [6,7] who, motivated by the structure of polyacetylene, considered a 1D dimerized chain of electrons (see also Refs. [8,9]). In their model, a Jakiw-Rebbi soliton carrying fractionalized quantum numbers [10] emerges at a domain wall between the two dimerization states. The Jakiw-Rebbi soliton state plays an important role in the theory of topological insulators [11,12]. Jakiw-Rebbi zero modes and geometric Zak phases [13] were observed in photonic and cold atomic systems [14–16]. However, a direct observation of a Jackiw-Rebbi (JR) soliton state and its fractional charge in solid state systems is lacking.

In this work, we propose a simple, robust experiment realizing JR fractionally charged states in carbon nanotubes (CNT). The suggested experimental setup [Fig. 1(a)] consists of a suspended metallic CNT touching a wedge-shaped pillar near its middle. A metallic CNT has a 1D Dirac electronic dispersion [17]. However, intrinsic tension shifts the quantization condition of the perpendicular momentum away from the Dirac point, opening a small gap (∼1–100 meV) [18,19]. By applying a magnetic field parallel to the CNT axis it is possible to shift the quantization condition such that the gap closes and reopens after crossing the Dirac point [20–22]. Since the strain on

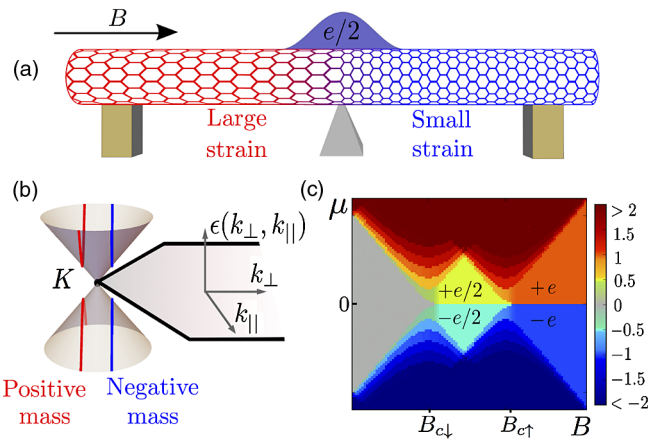

FIG. 1. (a) The proposed system. A suspended CNT is placed on a wedge-shaped pillar, causing the strain of the CNT at the left side(red) to be different then at the right side(blue). An axial magnetic field is applied. At a certain range of field, a Jackiw-Rebbi soliton state with a fractionalized charge is formed in the middle region. (b) The energy dispersion of the CNT can be understood as a 1D cut through the dispersion of the honeycomb lattice. The position of the cut depends on strain and magnetic field. Thus, as the field is varied, one of the CNT sub-bands may cross through the Dirac point, changing the sign of its mass term. (c) Predicted charge in the middle third of the CNT, as a function of magnetic field, B, and chemical potential, μ. (See text for details of the simulation.) In a range of fields and chemical potentials, the charge is $\pm e/2$; at higher fields, a spin-charge separated state with charge $\pm e$ and spin zero is formed.

both sides of the wedge is generically different, the gap in these two regions closes at different fields. Thus, there is a range of magnetic fields where the Dirac masses in the two regions *have an opposite sign* [Fig. 1(b)]. In this range, a robust SSH-like soliton state carrying a fractionalized charge emerges at the interface.

Figure 1(c) shows the predicted charge stability diagram. The color map represents the charge integrated over a region around the wedge, vs the axial magnetic field, B, and chemical potential, μ. For μ near the middle of the CNT's semiconducting gap, there are three regions of B: $B < B_{c\downarrow}$, where the charge is zero [$B_{c\downarrow}$ is the field of the topological transition for spin $\downarrow$ electrons, see Eq. (3)]; $B_{c\downarrow} < B < B_{c\uparrow}$, where the charge is $\pm e/2$; and $B_{c\uparrow} < B$, where the system exhibits "spin-charge separation": the charge is $\pm e$, while the spin is zero. $B_{c\downarrow}$ and $B_{c\uparrow}$ are different due to spin-orbit coupling in the CNT; this effect is crucial for realizing the $\pm e/2$ state.

As we will show below, the precise quantization of the charge localized in the middle region of the CNT in units of $e/2$ is a consequence of the symmetry of the CNT under a rotation by π followed by time reversal. Both chiral and nonchiral CNTs exhibit such symmetry.

For $B_{c\downarrow} < B < B_{c\uparrow}$, a precisely quantized fractional charge appears also *at the edge* of the CNT (see [23]). In-gap edge states may appear, as well [24,25]. Our setup has the advantage that the fractional charge is realized near the CNT's middle; the bulk is cleaner and better controlled than the edges. Moreover, in our setup the soliton is far from any metallic contacts that bend the CNT's bands due to the difference in work function, masking the fractional charge.

Carbon nanotunbe model.—The low-energy effective Hamiltonian of a CNT is given by $h(\boldsymbol{k}) = \hbar v_F(\xi\sigma_x k_x + \sigma_y k_y)$. Here, v_F is the Dirac velocity, σ_x, σ_y are Pauli matrices acting in the sublattice (A-B) space, and $\xi = +1(-1)$ corresponds to the K' (K) valley, respectively.

The CNT is specified by the chiral vector, $\boldsymbol{c} = n_1\boldsymbol{a_1} + n_2\boldsymbol{a_2}$, denoted by $c = (n_1, n_2)$, which connects two carbon atoms of the parent graphene sheet [26]. The perpendicular momentum to the tube is quantized due to its finite diameter. In an ideal metallic CNT ($n_1 - n_2 \in 3\mathbb{Z}$), the lines of allowed momenta cross the K, K' points. An axial magnetic field B and curvature effects in CNTs shift the allowed momenta lines away from K, K' [18,27]. The low-energy Hamiltonian takes the form [19]

$$h(k_\parallel) = \hbar v_F\left(\xi\sigma_x\frac{2\pi\phi}{|\boldsymbol{c}|\phi_0} + \sigma_y k_\parallel\right) + \delta t\sigma_x - (\Delta_o^{SO}\sigma_x + \Delta_z^{SO})\xi S_z. \quad (1)$$

Here, $\phi = Ba^2(|\boldsymbol{c}|/2\pi)^2$ is the flux through the CNT (a is the lattice spacing), $\phi_0 = h/e$, $k_\parallel$ is the momentum parallel to the CNT, S_z is the spin along the CNT axis, Δ_o^{SO}, Δ_z^{SO} are the strengths of the orbital and Zeeman-type spin-orbit couplings, respectively [19], and the δt term is due to strain along the axis of the CNT. The Δ_o^{SO}, Δ_z^{SO}, and δt terms are induced by curvature [19,28–31]. δt can be modified by applying external strain to the CNT [27]. We have neglected Zeeman coupling, which is smaller than the terms in Eq. (1).

Soliton states and fractional charges.—We now consider the system in Fig. 1(a). We focus on the case of a zigzag CNT with chiral vector $(N, 0)$. Similar considerations hold for other chiralities (see below). The tensile strain of the CNT is spatially inhomogeneous, and hence the δt term in Eq. (1) is $x_\parallel$ dependent (where $x_\parallel$ is the coordinate along the CNT). The wedge is at $x_\parallel = 0$. Across the wedge, δt varies; we assume for simplicity that $\delta t(x_\parallel)$ is piecewise constant, and denote the values of δt at $x_\parallel < 0$ ($x_\parallel > 0$) by δt_- (δt_+), respectively.

Then, the effective Hamiltonian is written as

$$H = \int dx_\parallel \left[m(\xi, S_z, x_\parallel)\sigma_x + \hbar v_F\sigma_y\left(-i\frac{\partial}{\partial x_\parallel}\right)\right], + \Delta_z^{SO}\xi S_z, \quad (2)$$

where $m(\xi, S_z, x_\parallel) = \hbar v_F(2\pi\phi/|\boldsymbol{c}|\phi_0)\xi - \Delta_o^{SO}\xi S_z + \delta t(x_\parallel)$. Equation (2) is equivalent to the JR problem [5]. For $\phi = 0$, m is generically nonzero for both valleys, $\xi = \pm 1$, and in either side of the wedge. As the magnetic field increases, there is a sequence of topological phase transitions where m goes through zero. For a certain range of magnetic field, the masses in the two spatial region have an opposite sign for either one or both spin flavors [see Figs. 2(a) and 2(b)]. Whenever the mass of one of the spin or valley bands has an opposite sign in the two regions, there is a localized state at the interface with an associated charge of $\pm e/2$ [5].

Figure 2(c) shows the spectrum as a function of magnetic field. We have assumed that $\delta t_- > \delta t_+ > \Delta_o^{SO} > \Delta_z^{SO} > 0$. The first two gap closing points occur for the spin up and down bands of valley K at $x_\parallel > 0$. The corresponding critical magnetic fields for spin $S_z = \uparrow, \downarrow$ are

$$B_{c,S_z} = \frac{2\pi\phi_0}{|\boldsymbol{c}|\hbar v_F}(\delta t_+ + \Delta_o^{SO}S_z). \quad (3)$$

For $B_{c\downarrow} < B < B_{c\uparrow}$, there is a single JR soliton state localized around the interface. The localization length is $\ell \sim v_F/m(x_\parallel)$, where $m(x_\parallel)$ is the mass at valley K and spin $\downarrow$ at either $x_\parallel > 0$ or $x_\parallel < 0$. Note that there is a different decay length to the left and to the right of the wedge. If the chemical potential is in the bulk gap, there is a well-defined charge of $\pm e/2$ distributed around the interface. The existence of a gap in the spectrum for $B_{c\downarrow} < B < B_{c\uparrow}$ requires that $\Delta_o^{SO} > \Delta_z^{SO}$. The ratio of Δ_o^{SO} and Δ_z^{SO} depends on the chiral vector of the CNT (see below).

For $B > B_{c\uparrow}$, but below the field in which the first topological phase transition occurs at $x_\parallel > 0$, there are *two* soliton states bound to the interface, one for each spin.

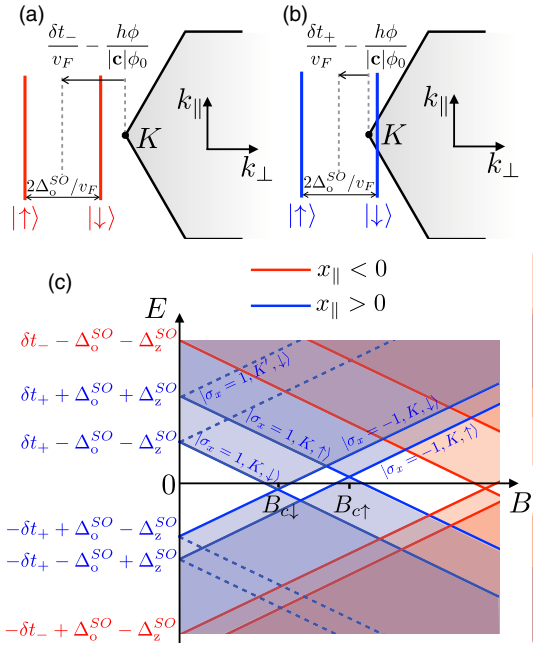

FIG. 2. (a),(b) Quantization lines of the perpendicular momentum around the K point for a zigzag CNT, shown in the honeycomb lattice Brillouin zone. The allowed values of $k_\perp$ depend on the strain δt on the flux ϕ, and on the spin [see Eq. (1)]. The blue (red) lines correspond to $x_\parallel < 0$ ($x_\parallel > 0$), respectively. One of the quantized momenta can sweep through the Dirac point in one spatial region of the system (a) but not in the other (b). This results in a Jackiw-Rebbi soliton state and a fractional charge at the interface. (c) Evolution of the spectrum as a function of axial magnetic field. White regions correspond to a gap, while filled regions represent the bulk spectrum. Solid (dashed) lines correspond to the gaps of states at the K (K') valley. The gap closes, and the Dirac mass changes sign, at $B = B_{c\uparrow,\downarrow}$ for the K valley bands with spin up and down, respectively.

The charge at the interface can be either $-e$, 0, or e, depending on the chemical potential. Just as in the SSH chain [32], the state of the interface exhibits "spin-charge separation": the charge $\pm e$ state has spin zero, while the zero charge state has spin $\pm\hbar/2$. In the latter state, the spin degeneracy is lifted by the Δ_z^{SO} term.

The equivalence of our system to the SSH model can be understood microscopically; see [23].

Fractional charge from geometric phases.—The presence of a fractional charge at the domain wall can be understood as a consequence of a topological invariant: the Zak phase [13]. The Zak phase is related to the *charge polarization density*. Upon changing δt from δt_- to δt_+, the total change in the polarization, ΔP, is [33]

$$\Delta P = \frac{e}{2\pi}\sum_{n\in\mathrm{occ}}\int_{\delta t_-}^{\delta t_+} d(\delta t)\int dk_\parallel \mathrm{Im}\langle\partial_{k_\parallel} u^{(n)}_{k_\parallel,\delta t}|\partial_{\delta t} u^{(n)}_{k_\parallel,\delta t}\rangle. \tag{4}$$

Here, the $k_\parallel$ integral is over the first Brillouin zone (BZ), $|u^{(n)}_{k_\parallel,\delta t}\rangle$ is the Bloch wave function in band n, and the summation is over the occupied bands.

We can replace Eq. (4) by a 2D integral over the Berry curvature, $\mathcal{F}(\mathbf{k})$ in the BZ of the honeycomb lattice, with (k_x, k_y) replaced with $(k_\parallel, k_\perp)$, where $k_\perp = (\delta t/\hbar v_F) - \xi(2\pi\phi/|\boldsymbol{c}|\phi_0)$ [see Eq. (1)]. Here, $\mathcal{F}(\boldsymbol{k}) = \pi\delta(\boldsymbol{k}-\boldsymbol{K}) - \pi\delta(\boldsymbol{k}-K')$. Therefore, ΔP is nonzero if during the change of δt, the allowed momenta crosses one or more Dirac points. In this case, the change in polarization density is $e/2$ per Dirac point crossed. The change in the charge at the interface is $\Delta q = \int_{x_1}^{x_2} dx(\partial\Delta P/\partial x) = \Delta P(x_2) - \Delta P(x_1)$. Hence, it is also quantized in units of $e/2$.

The precise quantization of the polarization is due to a spatial symmetry of the CNT. A CNT with an axial magnetic field is invariant under a rotation by 180° around an axis perpendicular to the CNT axis, followed by time reversal [23]. We denote this symmetry operation by $\mathcal{R}_\pi$. Under $\mathcal{R}_\pi$, $P \to -P$; however, since P in a crystal is only defined modulo e, $P\mathrm{mod}e = -P\mathrm{mod}e$. Hence, the possible values for P are either 0 or $e/2$, and the charge at the interface is quantized in units of $e/2$. If the interface charge is $e/2$, an extra charge of $e/2$ appears at the end of the CNT.

Note that the system is symmetric under $\mathcal{R}_\pi$ for *any* chiral vector. In armchair CNTs, however, both Dirac points are always crossed together, and therefore the charge at the interface is an integer multiple of e.

Above, we have assumed that there is no term in the Hamiltonian that breaks the symmetry between the A and B sublattices [a σ_z term in Eq. (1)]. Such a term would break the $\mathcal{R}_\pi$ symmetry, and the charge at the interface can take any value [34]. Such a term may arise in CNTs if the A-B symmetry is spontaneously broken due to interactions [21,35,36].

Finally, we note that the $e/2$ interface charge is robust in the presence of disorder, as long as the bulk remains insulating and the symmetry under $\mathcal{R}_\pi$ is still maintained *on average*.

Numerical simulations.—In order to demonstrate the phenomena described above, we simulated a tight-binding model of a CNT [23]. The model includes nearest-neighbor and next-nearest-neighbor hopping [37], as well as Zeeman and orbital-type spin-orbit coupling. The effect of strain is modeled by increasing the hopping on each bond by $\tilde{\delta t}\cos^2(\alpha)$, where α is the angle between the direction of the bond and the chiral vector, c. $\tilde{\delta t}$ is taken to have the following spatial dependence: $\tilde{\delta t}(x_\parallel) = \tilde{\delta t}_- + (\tilde{\delta t}_+ - \tilde{\delta t}_-)/(1+e^{x_\parallel/d})$. We used $d = 10a$, where a is the lattice spacing [38].

Figure 1(c) shows the excess charge in the interface region, as a function of magnetic field and chemical potential, μ. The excess charge is summed over a region of length $L/3$ centered around the interface (where L is the CNT length). For the given parameters this length

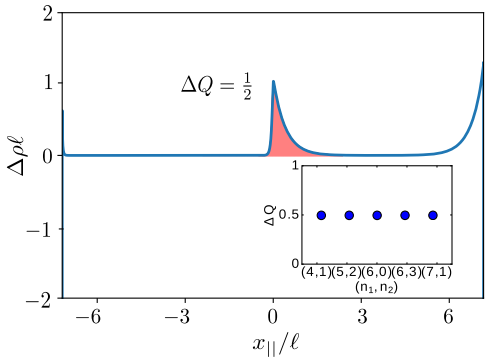

FIG. 3. Charge density vs position along the CNT, $x_\parallel$, for a $c = (6, 0)$ (zigzag) CNT [23]. The tight-binding parameters used are $\tilde{t} = 3$ eV, $\tilde{\delta t}_- = 14$ meV, $\tilde{\delta t}_+ = 84$ meV, $\tilde{\Delta}_o = 4$ meV, $\tilde{\Delta}_z = 0.4$ meV, $\tilde{\delta t}_{nnn} = 30$ meV. For these parameters, $\ell = \hbar v_F/\tilde{\Delta}_o \sim 0.2$ μm. Inset: the interface charge, ΔQ for CNTs with different chiral vectors.

corresponds to about $6\ell(B = B_0)$, where $\ell(B) = \hbar v_F/E_{\rm gap}(B)$ is the length scale associated with the gap $E_{\rm gap}(B)$ between the conduction and valence bands at $x_\parallel > 0$. The field B_0 was tuned such that $B_{c\downarrow} < B_0 < B_{c\uparrow}$. In this simulation, we set $\tilde{\Delta}_z^{SO} = 0$ for clarity; it is included in the following.

In Fig. 3 we show the excess charge density as a function of position, for a magnetic field $B_{c\downarrow} < B_0 < B_{c\uparrow}$, in a (6,0) zigzag CNT. Near the interface, there is a charge of $e/2$, localized over a region whose length is of the order of $\ell(B = B_0)$; another charge of $e/2$ is localized near the right end of the CNT. The inset shows the interface charge for CNTs with different chiral vectors; the charge is always $e/2$, independent of the chiral vector.

Discussion.—We now discuss considerations for an experimental realization of our proposed setup. References [20,39–41] demonstrated that it is possible to close and reopen a semiconducting gap in metallic CNTs using magnetic fields of a few Tesla. Realizing an interface charge of $e/2$ requires to drive *only one* spin species through the topological transition. In this case, the maximum gap is determined by the strength of the spin-orbit coupling in the CNT, which has been estimated to be of the order of $\Delta_{o,z}^{SO} \sim$ 0.08–1.7 meV [20,40–42]. Using $v_F \approx 10^6$m/s, we get that the interface charge is localized in a region of length $\ell \sim \hbar v_F/\Delta_o^{SO} \sim 0.35$–$7.5$ μm. Thus, our proposal requires a CNT whose length is a few μm. The possibility of fabricating long, pristine CNTs, and the detection of localized charges, have been demonstrated in Refs. [43,44].

To estimate the strain-induced gap in the CNT, we note that the tension at the contact with the wedge is expected to be ~10 nN [45]. Using the Young modulus of CNT, 0.1–1 T Pa [46], and the derivative of the energy gap with respect to strain, 100 meV/0.01 [18], the difference in the gap between the two regions is of the order of $\delta t_+ - \delta t_- \sim 1$–$10$ meV.

The existence of an interface charge of $e/2$ depends on the *type* of spin-orbit coupling in the CNT. Keeping the system insulating in the range of magnetic field where only one spin species has an inverted mass requires that the orbital-type spin orbit coupling, Δ_o^{SO}, is larger in magnitude than the Zeeman type term, Δ_z^{SO}. Theoretical considerations suggest that $\Delta_z^{SO} \sim \cos(3\theta)$, where θ is the chiral angle of the CNT [47], while Δ_o^{SO} does not depend on θ [30]. In particular, Δ_z^{SO} vanishes for an armchair CNT. Thus, the optimal chiral angle for realizing a charge of $e/2$ is close to $\theta = \pi/6$. This way, Δ_z^{SO} is small, while the K and K' points are still crossed at different magnetic fields.

An important practical challenge in observing the soliton state in our proposed setup is the need to maintain the chemical potential in the gap throughout the CNT. This can be done by using an array of metallic gates [43]. If the wedge is made of a metal covered by an oxide insulting barrier, it can be used as an additional gate that can tune the JR state to the Fermi level [23].

Finally, we comment on the effect of Coulomb interactions. As long as the interactions are not strong enough to drive the system through a phase transition, the value of the interface charge is fixed to an integer multiple of $e/2$. The length scale ℓ over which the localized charge decays becomes longer in the presence of interactions. However, a rough estimate shows that this effect is small for realistic interaction strengths [23]. In the presence of interactions, the induced charge density decays away from the wedge as $\rho_i \simeq \ell^{-1}(x_{||}/\ell)^{-3}$ [23], rather than exponentially.

We thank Y. Baum, I. C. Fulga, Y. Oreg, and M. S. Rudner for useful discussions. E. B. acknowledges support from a Marie Curie CIG grant and from the European Research Council (ERC) under the European Union Horizon 2020 research and innovation program (No. 639172). E. B. also thanks the hospitality of the Aspen Center for Physics, where part of this work was done. This work was supported in part by a grant from the Simons foundation. S. I. acknowledges financial support by the ERC Cog grant (See-1D-Qmatter, No. 647413).

[1] D. C. Tsui, H. L. Stormer, and A. C. Gossard, Two-Dimensional Magnetotransport in the Extreme Quantum Limit, Phys. Rev. Lett. **48**, 1559 (1982).
[2] R. B. Laughlin, Anomalous Quantum Hall Effect: An Incompressible Quantum Fluid with Fractionally Charged Excitations, Phys. Rev. Lett. **50**, 1395 (1983).
[3] R. de Picciotto, M. Reznikov, M Heiblum, V. Umansky, G. Bunin, and D. Mahalu, Direct observation of a fractional charge, Nature (London) **389**, 162.
[4] L. Saminadayar, D. C. Glattli, Y. Jin, and B. Etienne, Observation of the $e/3$ Fractionally Charged Laughlin Quasiparticle, Phys. Rev. Lett. **79**, 2526 (1997).
[5] R. Jackiw and C. Rebbi, Solitons with fermion number 1/2, Phys. Rev. D **13**, 3398 (1976).

[6] W. P. Su, J. R. Schrieffer, and A. J. Heeger, Solitons in Polyacetylene, Phys. Rev. Lett. **42**, 1698 (1979).
[7] W. P. Su, J. R. Schrieffer, and A. J. Heeger, Soliton excitations in polyacetylene, Phys. Rev. B **22**, 2099 (1980).
[8] M. J. Rice, Charged π-phase kinks in lightly doped polyacetylene, Phys. Lett. A **71**, 152 (1979).
[9] S. A. Brazovskiĭ and N. N. Kirova, Excitons, polarons, and bipolarons in conducting polymers, ZhETF Pisma Redaktsiiu **33**, 6 (1981).
[10] S. Kivelson and J. R. Schrieffer, Fractional charge, a sharp quantum observable, Phys. Rev. B **25**, 6447 (1982).
[11] M. Z. Hasan and C. L. Kane, Colloquium: Topological insulators, Rev. Mod. Phys. **82**, 3045 (2010).
[12] X.-L. Qi and S.-C. Zhang, Topological insulators and superconductors, Rev. Mod. Phys. **83**, 1057 (2011).
[13] J. Zak, Berry's Phase for Energy Bands in Solids, Phys. Rev. Lett. **62**, 2747 (1989).
[14] E. J. Meier, F. A. An, and B. Gadway, Observation of the topological soliton state in the Su-Schrieffer-Heeger model, Nat. Commun. **7**, 13986 (2016).
[15] T. Kitagawa, M. A. Broome, A. Fedrizzi, M. S. Rudner, E. Berg, I. Kassal, A. Aspuru-Guzik, E. Demler, and A. G. White, Observation of topologically protected bound states in photonic quantum walks, Nat. Commun. **3**, 882 (2012).
[16] M. Atala, M. Aidelsburger, J. T. Barreiro, D. Abanin, T. Kitagawa, E. Demler, and I. Bloch, Direct measurement of the Zak phase in topological bloch bands, Nat. Phys. **9**, 795 (2013).
[17] S. Ilani and P. L. McEuen, Electron transport in carbon nanotubes, Annu. Rev. Condens. Matter Phys. **1**, 1 (2010).
[18] E. D. Minot, Y. Yaish, V. Sazonova, and P. L. McEuen, Determination of electron orbital magnetic moments in carbon nanotubes, Nature (London) **428**, 536 (2004).
[19] J. Klinovaja, M. J. Schmidt, B. Braunecker, and D. Loss, Carbon nanotubes in electric and magnetic fields, Phys. Rev. B **84**, 085452 (2011).
[20] S. H. Jhang, M. Marganska, Y. Skourski, D. Preusche, B. Witkamp, M. Grifoni, H. van der Zant, J. Wosnitza, and C. Strunk, Spin-orbit interaction in chiral carbon nanotubes probed in pulsed magnetic fields, Phys. Rev. B **82**, 041404 (2010).
[21] V. V. Deshpande, B. Chandra, R. Caldwell, D. S. Novikov, J. Hone, and M. Bockrath, Mott insulating state in ultraclean carbon nanotubes, Science **323**, 106 (2009).
[22] H. B. Meerwaldt, G. Labadze, B. H. Schneider, A. Taspinar, Ya. M. Blanter, H. S. J. van der Zant, and G. A. Steele, Probing the charge of a quantum dot with a nanomechanical resonator, Phys. Rev. B **86**, 115454 (2012).
[23] See Supplemental Material at http://link.aps.org/supplemental/10.1103/PhysRevLett.119.147704 for further details about the tight binding model, the relation to the SSH chain, the $\mathcal{R}_\pi$ symmmetry, edge states in the presence of a uniform strain field, a method to maintain the chemical potential in the CNT's gap, and effects of interactions.
[24] L. Brey and H. A. Fertig, Electronic states of graphene nanoribbons studied with the dirac equation, Phys. Rev. B **73**, 235411 (2006).
[25] W. Izumida, R. Okuyama, A. Yamakage, and R. Saito, Angular momentum and topology in semiconducting single-wall carbon nanotubes, Phys. Rev. B **93**, 195442 (2016).
[26] S. Reich, C. Thomson, and J. Maultzsch, *Carbon Nanotubes: Basic Concepts and Physical Properties* (Wiley, New York, 2004).
[27] E. D. Minot, Y. Yaish, V. Sazonova, J.-Y. Park, M. Brink, and P. L. McEuen, Tuning Carbon Nanotube Band Gaps with Strain, Phys. Rev. Lett. **90**, 156401 (2003).
[28] T. Ando, Spin-orbit interaction in carbon nanotubes, J. Phys. Soc. Jpn. **69**, 1757 (2000).
[29] D. Huertas-Hernando, F. Guinea, and A. Brataas, Spin-orbit coupling in curved graphene, fullerenes, nanotubes, and nanotube caps, Phys. Rev. B **74**, 155426 (2006).
[30] J.-S. Jeong and H.-W. Lee, Curvature-enhanced spin-orbit coupling in a carbon nanotube, Phys. Rev. B **80**, 075409 (2009).
[31] W. Izumida, K. Sato, and R. Saito, Spin-orbit interaction in single wall carbon nanotubes: Symmetry adapted tight-binding calculation and effective model analysis, J. Phys. Soc. Jpn. **78**, 074707 (2009).
[32] A. J. Heeger, S. Kivelson, J. R. Schrieffer, and W. P. Su, Solitons in conducting polymers, Rev. Mod. Phys. **60**, 781 (1988).
[33] R. D. King-Smith and David Vanderbilt, Theory of polarization of crystalline solids, Phys. Rev. B **47**, 1651 (1993).
[34] E. J. Mele and Petr Král, Electric Polarization of Heteropolar Nanotubes as a Geometric Phase, Phys. Rev. Lett. **88**, 056803 (2002).
[35] R. Barnett, E. Demler, and E. Kaxiras, Superconducting and charge density wave instabilities in ultrasmall-radius carbon nanotubes, Solid State Commun. **135**, 335 (2005).
[36] M. Rontani, Anomalous magnetization of a carbon nanotube as an excitonic insulator, Phys. Rev. B **90**, 195415 (2014).
[37] The next-nearest-neighbor hopping terms are not essential for the realization of a fractional charge. We have verified that the interface charge remains precisely quantized if the next-nearest neighbor hopping term is set to zero.
[38] The simulations of chiral nanotubes were done using the Kwant package. See C. W. Groth, M. Wimmer, A. R. Akhmerov, and X. Waintal, Kwant: a software package for quantum transport, New J. Phys. **16**, 063065 (2014).
[39] K. Sasaki, S. Murakami, R. Saito, and Y. Kawazoe, Controlling edge states of zigzag carbon nanotubes by the aharonov-bohm flux, Phys. Rev. B **71**, 195401 (2005).
[40] F. Kuemmeth, S. Ilani, D. C. Ralph, and P. L. McEuen, Coupling of spin and orbital motion of electrons in carbon nanotubes, Nature (London) **452** (2008).
[41] G. A. Steele, F. Pei, E. A. Laird, J. M. Jol, H. B. Meerwaldt, and L. P. Kouwenhoven, Large spin-orbit coupling in carbon nanotubes, Nat. Commun. **4** (2013).
[42] T. S. Jespersen, K. Grove-Rasmussen, J. Paaske, K. Muraki, T. Fujisawa, J. Nygård, and K. Flensberg, Gate-dependent spin-orbit coupling in multielectron carbon nanotubes, Nat. Phys. **7**, 348 (2011).
[43] J. Waissman, M. Honig, S. Pecker, A. Benyamini, A. Hamo, and S. Ilani, Realization of pristine and locally tunable one-dimensional electron systems in carbon nanotubes, Nat. Nanotechnol. **8**, 569 (2013).
[44] A. Hamo, A. Benyamini, I. Shapir, I. Khivrich, J. Waissman, K. Kaasbjerg, Y. Oreg, F. von Oppen, and S. Ilani, Electron

attraction mediated by coulomb repulsion, Nature (London) **535**, 395 (2016).

[45] J. D. Whittaker, E. D. Minot, D. M. Tanenbaum, P. L. McEuen, and R. C. Davis, Measurement of the adhesion force between carbon nanotubes and a silicon dioxide substrate, Nano Lett. **6**, 953 (2006).

[46] K.-t. Lau, C. Gu, and D. Hui, A critical review on nanotube and nanotube/nanoclay related polymer composite materials, Composites Part B Engineering **37**, 425 (2006).

[47] θ is defined as the angle between the chiral vector of a CNT and a chiral vector corresponding to a zigzag CNT.